Journal of Iron and Steel Research, International 24 (2017) 536－543

Contents lists available at ScienceDirect

Journal of Iron and Steel Research, International

journal homepage: www.chinamet.cn

Effects of micro-alloying and production process on precipitation behaviors and mechanical properties of HRB600

Hong-bo Pan[1,2,*], Meng-jiao Zhang[3], Wei-ming Liu[1,2], Jun Yan[1,2], Hui-ting Wang[3], Chang-sheng Xie[3], Zhan Guo[4]

[1] Key Laboratory of Metallurgical Emission Reduction & Resources Recycling of Ministry of Education, Anhui University of Technology, Ma'anshan 243002, Anhui, China

[2] Anhui Province Key Laboratory of Metallurgy Engineering & Resources Recycling, Anhui University of Technology, Ma'anshan 243002, Anhui, China

[3] School of Metallurgical Engineering, Anhui University of Technology, Ma'anshan 243002, Anhui, China

[4] Technology Center, Ma'anshan Iron & Steel Company Limited, Ma'anshan 243000, Anhui, China

ARTICLE INFO

Key words:
Micro-alloying
High-strength steel rebar
Thermo-mechanical controlling process
Mechanical property
Precipitation strengthening
Thermodynamics

ABSTRACT

Effects of micro-alloying elements and production process on microstructure, mechanical properties and precipitates of 600 MPa grade rebars were studied by using pilot test, metallographic observation, tensile test, thermodynamic calculation and transmission electron microscopy. The results show that the tested steels are composed of ferrite and pearlite, in which the content range of pearlite is 33%－45%. For vanadium micro-alloyed steel, interphase precipitation strengthening effect of V can be promoted and the yield strength of tested steels can be increased with increasing V content and decreasing finishing rolling temperature. The temperature of terminated cooling should be more than 700 ℃ when the water cooling is used. When niobium is added to the steel, more coarse (Nb,V)C,N precipitates are generated at high temperature, so that the solid solubility of precipitated phases of vanadium is reduced and the precipitation strengthening effect of vanadium is weakened.

1. Introduction

In recent years, the production and consumption of hot-rolled steel rebar in China have been greatly increased with the rapid development of urbanization and construction industry. In accordance with the research data of Chinese industrial information, the total steel rebar production in 2013 has reached about 2.06×10^6 t[1]. Although the production of steel rebar in China has achieved rapid growth, their structures and varieties are in a relatively low level, wherein the amount of 400 MPa grade (grade III) steel rebars accounts for about 90% and the amount of above 500 MPa grade (grade IV) steel rebars accounts for less than 5%. On the contrary, 500 MPa grade steel rebars are widely used in developed countries, and the amount of 500－600 MPa grade steel rebars accounts for more than 95%. The United States, Britain, Germany, Australia, France and other major industrialized countries have developed 600 MPa grade high strength steel rebars and 700 MPa grade steel rebars are under active development. The ultra-high strength steel rebars whose yield strength is between 685 and 1275 MPa have been developed in Japan, to improve the seismic resistance of buildings and have already been applied in high-rise buildings[2]. Russia added 600 MPa grade steel rebars into steel product standard in 1993 and South Korea added 600－700 MPa high strength steel rebars into steel product standard in 2007[3]. However, for the construction of engineering projects with a huge building size, complex function and large infrastructure, such as high-rise and super high-rise buildings, long-span bridges, and undersea tunnel construction, the normal strength steel rebars used as the main materials of building structure are unable to meet the demand of weight-reduction and durability of the building, so that better performance and higher strength rebars are in urgent need. The use of high strength steel rebars can not only solve the problem of fat beams and columns of building structure, but also increase the usable construction area

* Corresponding author. Assoc. Prof., Ph.D.
E-mail address: *panhb718@163.com* (*H. B. Pan*).

Received 6 August 2016; Received in revised form 16 September 2016; Accepted 23 September 2016
Available online 15 May 2017

and make the structure design more flexible. Besides, compared with the mainly used 400 and 500 MPa grade steel rebars, 600 MPa grade high strength steel rebars can save steel consumption of 33.3% and 19.2% respectively, and have a practical significance for energy saving and emission reduction[3].

At present, the main production processes of high strength steel rebars are Tempcore treatment (TMT process) and micro-alloying. The TMT process has been commonly used to improve the strength of steel rebars in Europe, Russia, Australia and South Korea since the majority of them use steel binding rebars to connect[2,4]. India has also carried out a lot of researches and applications in TMT process[5,6]. Because of the common use of welding and sleeve connection in China, the main production process is micro-alloying with addition of Nb or V which can refine the grain and control the precipitation process to improve the strength and performance of steel rebars. In this study, trial test and transmission electron microscopy (TEM) were conducted to analyze the effect of micro-alloying and production process on the precipitation behaviors and mechanical properties of 600 MPa grade high strength rebars, which can provide theoretical support for the optimal design of the composition, process and industrial stable production.

2. Experimental Materials and Procedures

Three kinds of steels with different chemical compositions were designed to study the effects of Nb, V, and N contents on the strength and precipitation behaviors, and were then smelted by a 150 kg medium frequency induction melting furnace. The chemical compositions are listed in Table 1. The casting ingots were heated to 1200 ℃ and then forged into 180 mm×200 mm×80 mm (length×width×height) slab. Different finishing rolling temperatures and cooling modes were used, and the ingots were finally rolled to the target thickness of 10 mm (reduction ratio is 8) by a pilot two-high hot rolling mill and the specific process scheme was as follows: the ingots were heated to 1230 ℃, rolled with finishing rolling temperatures of 900 and 1000 ℃, and then cooled by air and water. Air cooling was carried out again after the ingot was cooled to the target temperature for simulating cooling bed. Actual processing parameters of tested steels are shown in Table 2.

Table 1
Chemical composition of tested steels (wt.%)

Steel grade	C	Si	Mn	P	S	Al_s	N	V	Nb	Fe
1	0.254	0.71	1.53	0.021	0.017	0.028	0.014	0.14	—	Balance
2	0.263	0.59	1.49	0.024	0.014	0.046	0.018	0.17	—	Balance
3	0.230	0.58	1.44	0.022	0.013	0.027	0.014	0.14	0.043	Balance

Table 2
Actual processing parameters of tested steels

Number	Finishing rolling temperature/℃	Cooling mode	Water cooling terminal temperature/℃
1-1	960－980	Air cooling	
1-2	930－950	Water cooling	690－760
1-3	900	Water cooling	680－740
2-1	980－1020	Air cooling	
2-2	1000	Water cooling	690－780
2-3	900	Water cooling	620－670
3-1	976	Air cooling	
3-2	960－980	Air cooling	
3-3	900	Air cooling	

Metallographic specimens were cut and embedded, then mechanically ground and polished. The microstructure was observed by using an OLYMPUS-BX51 optical microscope after etched with 4 vol.% nital. The ferrite grain size and pearlite content were quantitatively analyzed by Image-pro plus software while A_{80} non scale standard tensile specimens were cut from the rolled samples along the rolling direction and were performed in a Zwick/Roell Z020 tensile testing machine at room temperature according to Chinese standard GB/T 228.1-2010. The TEM observation samples were cut by wire-electrode, then mechanically ground to thin films of about 50 μm in thickness, and finally punched to prepare round disks of 3 mm in diameter. The disks were electropolished in a solution of 95 vol.% ethanol and 5 vol.% perchloric acid at －30 ℃ by using a twin-jet polisher with the operating voltage of 50 V. The precipitates were observed by a Philips TECNAI F30 field emission transmission electron microscope with an accelerating voltage of 300 kV.

The phase transition temperatures based on thermal expansion principle were measured with Gleeble 3500 thermal-mechanical simulation testing machine. The samples were cylinders with diameter of 6 mm and length of 90 mm, and were heated to 1000 ℃ at a heating rate of 0.1 ℃/s.

3. Results and Discussion

3.1. Mechanical properties

Mechanical properties of tested steels are shown in Table 3, where the values are the average results of

Table 3
Mechanical properties of tested steels

Number	R_{eL}/MPa	R_m/MPa	A_{gt}/%	A_{80}/%
1-1	604.3	791.5	10.97	24.52
1-2	629.5	804.9	10.75	18.56
1-3	677.8	858.3	8.57	15.94
2-1	643.4	833.4	10.14	22.91
2-2	652.9	838.7	9.97	18.39
2-3	559.6	733.7	9.46	15.31
3-1	588.5	785.7	11.14	22.88
3-2	582.7	765.9	11.91	21.94
3-3	580.4	757.4	11.90	21.59
GB1499.2-2013 standard requirements	≥600	≥730	≥7.50	≥14.00

Note: R_{eL}—Yield strength; R_m—Tensile strength; A_{gt}—Uniform elongation; A_{80}—Percentage elongation.

two tensile samples tested under the same condition. It can be seen that under the experimental conditions, the tensile strength, uniform elongation and percentage elongation all meet the standard of GB1499.2-2013 while the yield strength does not meet it in the sample Nos. 2－3 of vanadium micro-alloyed steels and all samples of Nb-V micro-alloyed steels. Besides, the high uniform elongation and percentage elongation also meet the requirements of the HRB600E seismic reinforcement.

3.2. Microstructure

In order to investigate the influence of water cooling on the microstructure of tested steels, the microstructures of surface with and without water cooling were analyzed. Figs. 1－3 show the microstructures of tested steels under diverse process conditions. It can be seen that the microstructure is composed of ferrite and pearlite, and there is no bainite and martensite under all conditions. In accordance with the pearlite content in Fig. 4 and mechanical properties in Table 3, it can be found that the mechanical properties are incompletely corresponding to the pearlite content even if they have the same composition. Combined the ferrite grain size in Fig. 5 with mechanical properties in Table 3, it can be found that the

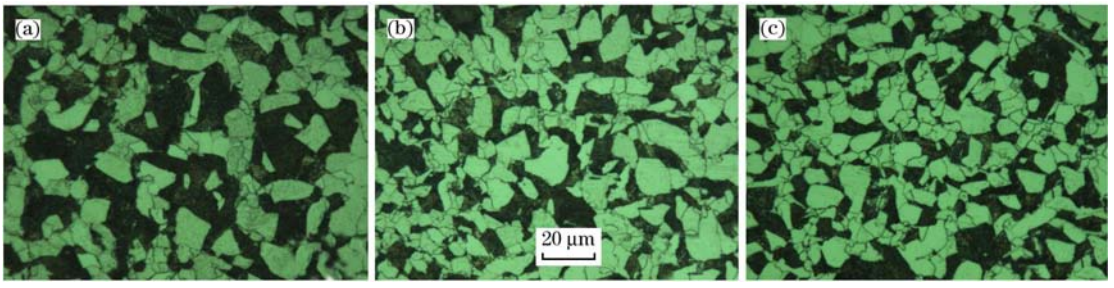

(a) 1-1; (b) 1-2; (c) 1-3.
Fig. 1. Microstructure of tested steel No. 1 under different processes.

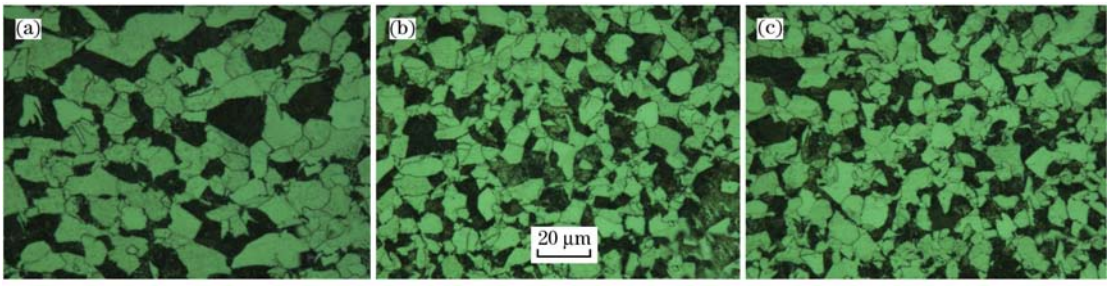

(a) 2-1; (b) 2-2; (c) 2-3.
Fig. 2. Microstructure of tested steel No. 2 under different processes.

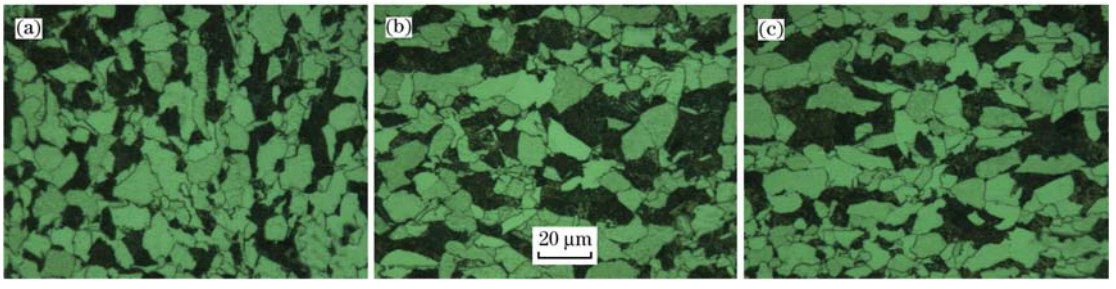

(a) 3-1; (b) 3-2; (c) 3-3.
Fig. 3. Microstructure of tested steel No. 3 under different processes.

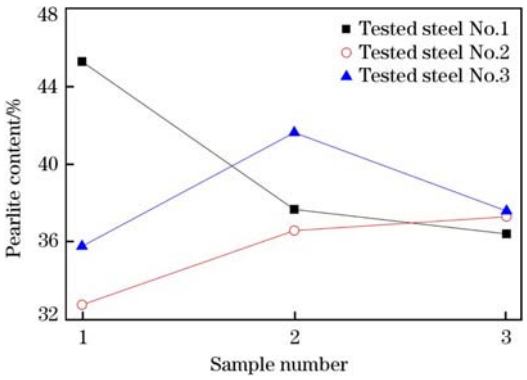

Fig. 4. Pearlite content of tested steels under different processes.

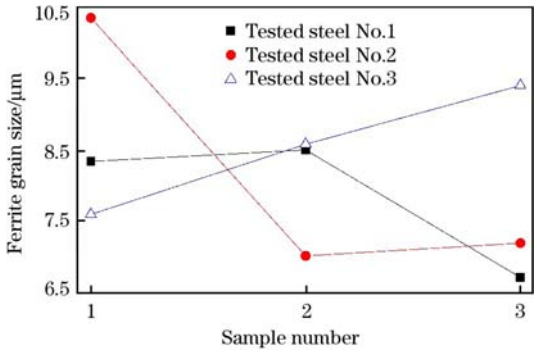

Fig. 5. Ferrite grain size of tested steels under different processes.

grain size and yield strength of tested steels do not strictly conform to the Hall-Petch relationship. Based on the above conclusions, the strengthening ways of tested steels which play a decisive role in determining the strength are neither solid solution strengthening, phase transformation hardening, nor grain refinement strengthening, but others.

3.3. Precipitate particles morphology

The precipitates morphology and distribution in the ferrite matrix and in the interior of pearlite of the specimen No. 1-1 are shown in Figs. 6(a) and 6(b), respectively. It can be seen that in Fig. 6(b), the precipitates basically appear as a whole in the morphology of small and sparse particles except partially coarsening precipitates in the ferrite matrix. Fig. 6(c) presents the interphase precipitation morphology of specimen No. 1-3, which indicates that the precipitates are distributed uniformly and densely in the ferrite matrix, while Fig. 6(d) presents the dislocation morphology of specimen No. 1-3 and shows that fine precipitates appear near the dislocation.

Fig. 7(a) presents the precipitates morphology distribution of V(C,N) and diffraction pattern of the matrix in the specimen No. 2-1. It can be seen that the precipitates in parallel exhibit the typical interphase precipitation mechanism, in which some fine precipitates in short rod-like shape are connected with

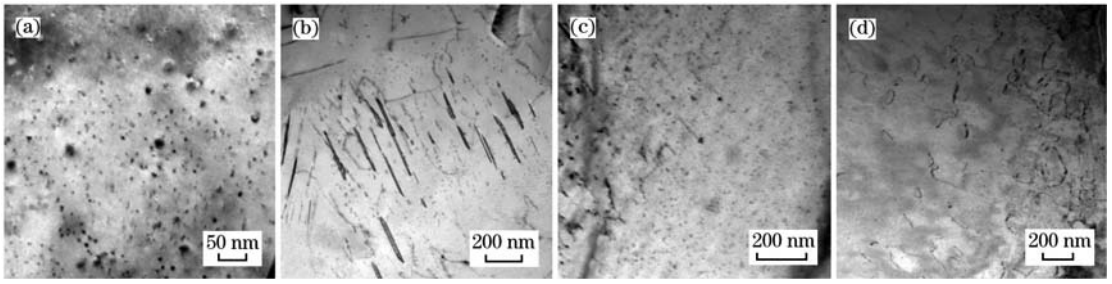

(a),(b) 1-1; (c),(d) 1-3.

Fig. 6. Precipitates distribution and dislocation morphology of tested steel No. 1 under different processes.

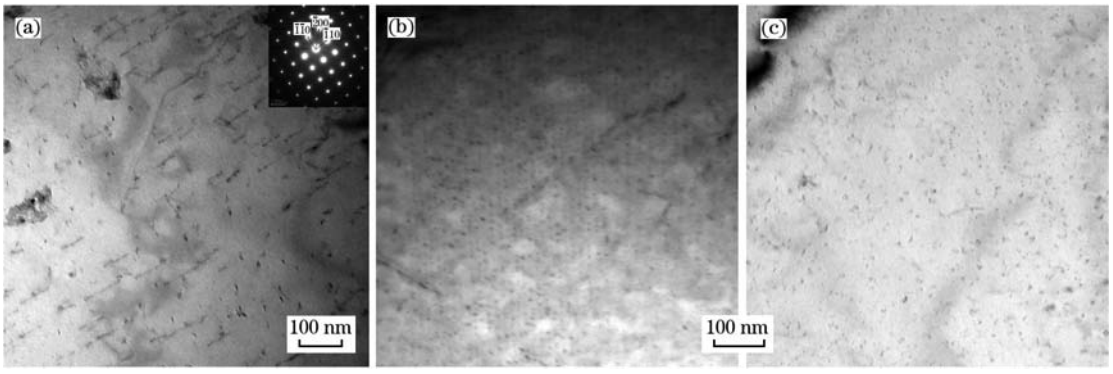

(a) 2-1; (b) 2-2; (c) 2-3.

Fig. 7. Precipitates distribution of tested steel No. 2 under different processes.

each other. Fig. 7(b) presents the precipitates distribution of V(C, N) in the specimen No. 2-2, from which it can be seen that the dispersive and fine precipitates in parallel with smaller space between two parallel precipitates are distributed in the ferrite matrix densely. Likewise, Fig. 7(c) presents the precipitates distribution of V(C, N) in the specimen No. 2-3, indicating that the dispersive and fine precipitates are relatively sparse and distributed randomly in the ferrite matrix.

The precipitates of the specimen No. 3-2 are composed of short rod-like, round-like, square-like and fine dispersively distributed dot-like particles as illustrated in Fig. 8(a). The energy spectrum analysis results demonstrate that the length of about 200 nm short rod-like and about 25 nm small square-like precipitates (as indicated by A in Fig. 8(a)) are (Nb,V) complex precipitates. Fig. 8(d) shows the energy dispersive spectrometry (EDS) analysis result. Similarly, the diameter of about 100 nm circular precipitates (as indicated by B in Fig. 8(a)) is (Nb, V, Ti) compound precipitates and its EDS spectrum is shown in Fig. 8(e). Besides, titanium element may be brought from smelting scrap materials. The dispersive and fine particles (as indicated by C in Fig. 8(a)) are V(C,N) precipitates whose EDS spectrum is shown in Fig. 8(f). Fig. 8(b,c) presents the precipitates distribution of the specimen No. 3-3, and it can be seen that the precipitates are composed of round-like and small particles. Fig. 8(g) presents the compound precipitation of Nb, V and Ti which appeared as circular precipitates of 100 nm in diameter (as indicated by D in Fig. 8(c)) and then titanium element may be brought from smelting scrap. Precipitates of V(C, N) distribute sparsely in the ferrite matrix (as shown in Fig. 8(b)), and some of

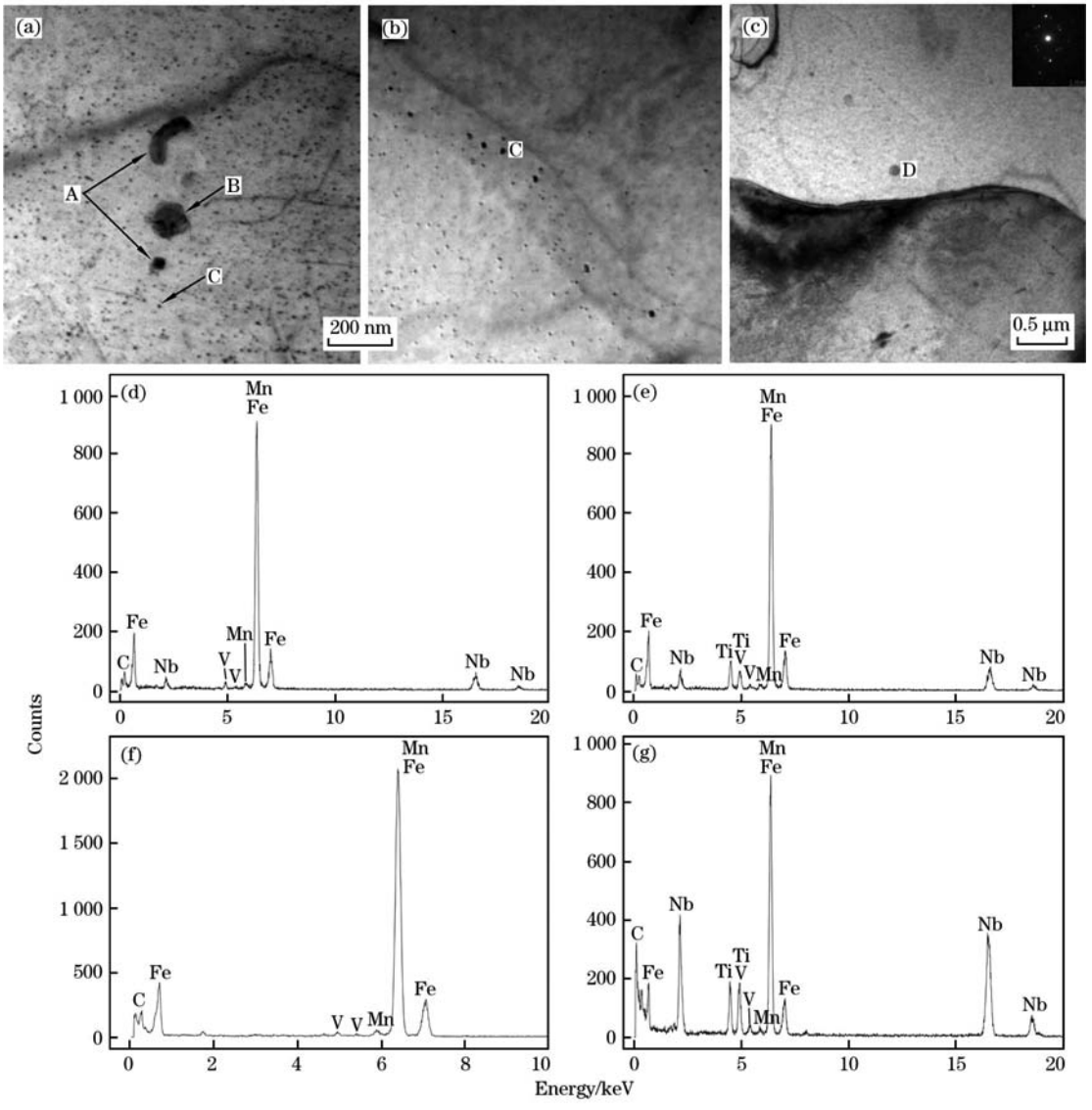

(a) 3-2; (b),(c) 3-3; (d)－(g) EDS of particles A, B, C and D respectively.

Fig. 8. Precipitates distribution and EDS analysis of tested steel No. 3 under different processes.

them are coarsened (as indicated by C in Fig. 8(b)).

3.4. Analysis and discussion

Precipitation hardening of micro-alloying elements is the primary strengthening mode in high-strength steel rebars. Micro-alloying elements Nb and V exist in the form of solid solution and precipitates to refine the microstructure and improve the strength by hindering the recrystallization and austenite grain growth. Moreover, their carbide and nitride precipitates (or carbonitrides) play an important role in improving the mechanical properties of the steel[7]. Table 4 presents the solid solubility formulae of the precipitated phases in the austenite.

Table 4
Solid solubility equation of different precipitated phases

Precipitated phase	Solid solubility equation
NbN	$\lg w_{[Nb]}w_{[N]}=2.80-8500/T$[8]
NbC	$\lg w_{[Nb]}w_{[C]}=3.42-7900/T$[9]
Nb(C,N)	$\lg w_{[Nb]}(w_{[C]}+12/14w_{[N]})=2.26-6770/T$[10]
VN	$\lg w_{[V]}w_{[N]}=3.46-8330/T$[11]
VC	$\lg w_{[V]}w_{[C]}=6.72-9500/T$[11]

There are three precipitation ways to over-saturated Nb and V in the process of rolling and cooling: (1) precipitated from austenite during the hot rolling in the form of carbides, nitrides or carbonitrides, (2) precipitated from the phase boundary (interphase precipitation) during the cooling transformation, and (3) precipitated from the over-saturated ferrite[12,13]. According to the thermodynamics, niobium has lower solid solubility and higher precipitation temperature than vanadium in accordance with the solid solubility equations given in Table 4. The range of precipitation temperature is shown in Fig. 9, in which precipitation starting temperature is defined as a temperature with 5% precipitation while precipitation finishing temperature is defined as a temperature with 95% precipitation. The phase transition temperatures measured at the heating rate of 0.1 ℃/s are used as a quasi-equilibrium phase transition temperatures. The quasi-equilibrium phase transition temperatures of tested steels from thermal expansion are shown in Table 5. It can be seen from Fig. 9 and Table 5 that the carbides and nitrides (or carbonitrides) of niobium are mainly precipitated in the austenite while those of vanadium are precipitated in

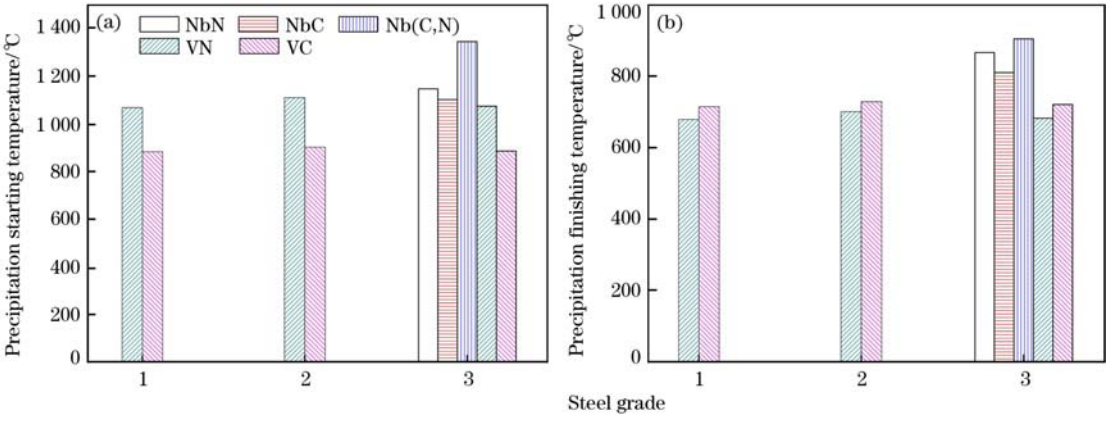

(a) Precipitation starting temperature; (b) Precipitation finishing temperature.

Fig. 9. Precipitation temperatures of different precipitation phases of tested steels.

Table 5
Quasi-equilibrium phase transition temperatures of tested steels

Steel grade	A_{c1}/℃	A_{c3}/℃
1	722.3	794.5
2	716.6	791.4
3	723.4	797.0

Note: A_{c1} and A_{c3} are pearlite to austenite and ferrite to austenite quasi-equilibrium phase transition temperatures, respectively.

the phase boundary during the austenite to ferrite transformation as well as in the ferrite after phase transformation. Nevertheless, the strengthening effect mainly comes from the particles which partially keep coherent with the matrix and are precipitated in the ferrite during or after the austenite to ferrite transformation. The carbides and nitrides (or carbonitrides) precipitated from the austenite can play a certain role in grain refinement, whereas they may reduce the solid solubility of the micro-alloying elements and precipitates in the ferrite and the phase boundary, and then decrease the yield strength. Besides, it can be seen from the comparison between the mechanical properties given in Table 3 and precipitates shown in Fig. 8 that relatively coarse Nb(C,N) precipitates are formed at higher temperature because of the addition of niobium, which results in the reduction of the nitrogen content combined with the vanadium content and strengthening effect of vanadium precipitation. This is the reason for the yield

strength decrease of tested steel No. 3.

It can be seen from Fig. 9 that the precipitation temperature range of VN is larger than that of VC, that is to say, it has a greater chemical driving force in the formation of VN considering from the thermodynamics. Each addition of 0.001% nitrogen in vanadium micro-alloyed steel can result in a strength increment of about 6 MPa. The addition of nitrogen can not only accelerate the precipitation of V(C,N), but also reduce the average diameter of V(C,N) particles and increase the volume fraction of fine particles significantly[14,15]. At the same time, the addition of micro-alloying elements also increases the whole solid solution temperature, enlarges the high precipitation temperature region and significantly increases the amount of precipitates in the process of temperature drop[16]. The combination of chemical composition given in Table 1, mechanical properties shown in Table 3 and precipitates shown in Fig. 7(a,b) illustrate that the addition of vanadium and nitrogen increases the precipitations of fine VN, VC and V(C,N), improves the precipitation strengthening effect and consequently results in relatively higher yield strength. The carbides (or nitrides) of vanadium precipitated from the interphase and the over-saturated ferrite in TMCP (thermo-mechanical control process) have striking precipitation strengthening effect. It has been studied that precipitation of vanadium precipitates is not only related to the alloying elements content, but also has a great relationship with the cooling process[17]. Moreover, it can also be seen from the thermodynamic calculation results given in Fig. 9 that V(C,N) precipitates of tested steel No. 2 begin to precipitate when the temperature reaches between 1000－1100 ℃ and the nose temperature of the shortest precipitation time is about 820 ℃[18]. In conclusion, because of the higher cooling intensity or faster cooling rate (specimen No. 2-3 shown in Table 2) during the cooling process, the residence time of the steel at high temperature was too short to fully precipitate carbonitrides of vanadium that mostly exist in the steel in the form of solid solution (as shown in Fig. 7(c)), which results in the weakening of the strengthening effect of vanadium precipitation and the reduction of the yield strength of specimen No. 2-3.

According to the study proposed by Bepari[19], interphase precipitation and dispersed precipitation exist at the same time in the continuous cooling process of the steel containing 0.2% vanadium, and interphase precipitation corresponds to the slower cooling rate; however, dispersed precipitation corresponds to the lower vanadium content (less than 0.1%)[20]. It can be seen from the combination of the chemical composition given in Table 1 and precipitates shown in Fig. 6(a) that dispersed precipitation is the main precipitation way in the tested steel of the specimen No. 1-1 rather than interphase precipitation, so that the vanadium precipitation is not sufficient to improve the yield strength as shown in Table 3. Nevertheless, the low temperature deformation of the steel can increase the dislocation intensity and vacancies, and then increase the nucleation position and diffusion coefficient of precipitation forming elements, which result in the acceleration of the precipitation process[21]. Furthermore, it can be seen from the process parameters given in Table 2 that the tested steel of the specimen No. 1-3 has relatively lower deformation temperature and an appropriate cooling rate, which promote the formation of precipitates and refinement as shown in Fig. 6(c); on the other hand, some precipitates are precipitated near the dislocations and pin dislocations as shown in Fig. 6(d). These two aspects make the yield strength to be improved greatly.

4. Conclusions

(1) The microstructure of three kinds of HRB600 is composed of ferrite and pearlite, in which the pearlite content is 33%－45%. For V-bearing high strength steel rebars, the yield strength of steel rebars satisfies the requirement of Chinese standard GB1499.2 when the cooling finishing temperature is controlled above 700 ℃ under water cooling condition. The yield strength of (Nb,V) micro-alloyed high strength steel rebars does not satisfy that standard under air cooling condition.

(2) For a V-bearing high strength steel rebar, the yield strength increases with decreasing finishing rolling temperature and increasing cooling rate. Too much cooling intensity is detrimental to the complete precipitation of vanadium and makes precipitates become sparse and fine. Different precipitation ways correspond to different conditions. When the vanadium content is less than 0.15%, dispersion precipitation corresponds to the condition with higher finishing rolling temperature and lower cooling rate, while interphase precipitation corresponds to the condition that the finishing rolling temperature is as low as 900 ℃ with the slow cooling near the ferrite transformation temperature. When the vanadium content is more than 0.15%, dispersion precipitation corresponds to the condition with lower finishing rolling temperature and faster cooling rate while interphase precipitation corresponds to the condition with the slow cooling near the ferrite transformation temperature.

(3) In the (Nb,V) composite micro-alloyed high strength steel rebar, precipitates are mainly composed of coarse carbonitride compounds in the size of 100－200 nm and in the form of short rod-like, round-like and square-like shapes. The precipitation

temperature of niobium is above 900 ℃, so that the steel rebars are rolled in a finishing rolling temperature between 900－1000 ℃, and then is cooled in air. Herein, this production process has little influence on the mechanical properties of tested steel.

Acknowledgment

This research was supported by Natural Science Research Project of Anhui Province of China (KJ2016A091), Natural Science Foundation of Anhui Province (1708085ME116), and Science and Technology Research Program of Anhui Province of China (1201a0201005).

References

[1] H. W. Kuang, W. Pan, L. Y. Ye, Ind. Const. 46 (2016) 620-626 (in Chinese).
[2] C. F. Yang, Iron and Steel 45 (2010) No. 11, 1-11 (in Chinese).
[3] J. W. Pan, Experimental Research on Mechanical Properties of 600 MPa Steel Bars under High Temperature, Qingdao University of Technology, Qingdao, 2015 (in Chinese).
[4] H. Khalifa, G. M. Megahed, R. M. Hamouda, M. A. Taha, J. Mater. Process. Technol. 230 (2016) 244-253.
[5] M. Mukherjee, C. Dutta, A. Haldar, Mater. Sci. Eng. A 543 (2012) 35-43.
[6] S. K. Paul, S. Majumdar, S. Kundu, Mater. Des. 58 (2014) 402-411.
[7] X. D. Huo, L. J. Li, Z. W. Peng, S. J. Chen, J. Iron Steel Res. Int. 23 (2016) 593-601.
[8] Q. Y. Zhang, J. Zhang, G. P. Liu, L. T. Wang, in: CSM, Baosteel Group Corp. (Ed.), Proceedings of the 10th CSM Steel Congress & the 6th Baosteel Biennial Academic Conference, Metallurgical Industry Press, Shanghai, 2015, pp. 1-8.
[9] H. L. Wei, G. Q. Liu, Mater. Des. 56 (2014) 437-444.
[10] S. Ghosh, A. K. Singh, S. Mula, P. Chanda, V. V. Mahashabde, T. K. Roy, Mater. Sci. Eng. A 684 (2017) 22-36.
[11] C. F. Yang, Y. Q. Zhang, R. Z. Wang, The Principle and Application of Vanadium Steel Metallurgy, Metallurgical Industry Press, Beijing, 2012 (in Chinese).
[12] F. Z. Bu, X. M. Wang, S. W. Yang, C. J. Shang, R. D. K. Misra, Mater. Sci. Eng. A 620 (2015) 22-29.
[13] P. Gong, E. J. Palmiere, W. M. Rainforth, Acta Mater. 97 (2015) 392-403.
[14] Y. Guan, X. Z. Zhang, J. Y. Ma, Adv. Mater. Res. 311-313 (2011) 817-821.
[15] C. F. Yang, Q. L. Wang, J. Iron Steel Res. Int. 15 (2008) No. 2, 81-86.
[16] L. Qi, A. M. Zhao, Z. Z. Zhao, Y. Huang, Mater. Sci. Technol. 20 (2012) No. 6, 29-34 (in Chinese).
[17] T. N. Baker, Mater. Sci. Technol. 25 (2009) 1083-1107.
[18] F. Fang, Q. L. Yong, C. F. Yang, H. Su, J. Iron Steel Res. Int. 17 (2010) No. 2, 36-42.
[19] M. A. Bepari, Metall. Trans. A 21 (1990) 2839-2855.
[20] S. Shanmugam, R. D. K. Misra, T. Mannering, D. Panda, S. G. Jansto, Mater. Sci. Eng. A 437 (2006) 436-445.
[21] S. F. Medina, Acta Mater. 84 (2015) 202-207.